Essential role of Flk-1 (VEGF receptor 2) tyrosine residue 1173 in vasculogenesis in mice

Yoshiko Sakurai*, Kaori Ohgimoto*, Yuki Kataoka†, Nobuaki Yoshida†, and Masabumi Shibuya*‡

Divisions of *Genetics and †Gene Expression and Regulation, Institute of Medical Science, University of Tokyo, 4-6-1 Shirokane-dai, Minato-ku, Tokyo 108-8639, Japan

Edited by Joseph Schlessinger, Yale University School of Medicine, New Haven, CT, and approved December 8, 2004 (received for review July 12, 2004)

Flk-1 (human counterpart, KDR) tyrosine kinase, which is one of the two VEGF receptors, is crucial for vascular development. Recently, we showed that, among tyrosine residues of KDR, tyrosine residues 1175 (Y1175, corresponding to Y1173 in murine Flk-1) and Y1214 (Y1212 in Flk-1) are autophosphorylated in response to VEGF, and that Y1175 is important for VEGF-dependent phospholipase Cγ/PKC/mitogen-activated protein kinase activation leading to DNA synthesis in cultured endothelial cells. However, the importance of these tyrosine residues in Flk-1/KDR *in vivo* is not yet known. To examine the role of these Flk-1 tyrosine residues *in vivo*, we generated knock-in mice substituting Y1173 and Y1212 of the *Flk-1* gene with phenylalanine, respectively. As a result, *Flk-1*^{1173F} homozygous mice died between embryonic days 8.5 and 9.5 without any organized blood vessels or yolk sac blood islands, and hematopoietic progenitors were severely reduced, similar to the case of *Flk-1* null mice. In contrast, *Flk-1*^{1212F} homozygous mice were viable and fertile. These results suggest that the signaling via Y1173 of Flk-1 is essential for endothelial and hematopoietic development during embryogenesis.

Flk-1/KDR | single tyrosine–phenylalanine mutation | tyrosine kinase receptor

VEGF is essential for many angiogenic processes both in normal and pathological conditions (1, 2). VEGF binds two tyrosine kinase receptors, Flt-1 (also known as VEGF receptor 1) (3, 4) and Flk-1 (also known as VEGF receptor 2, KDR as human counterpart) (5–7) with high affinity. *Flt-1*- and *Flk-1*-deficient mice both die *in utero* between embryonic days (E) 8.5 and E9.5 but have different phenotypes. *Flt-1*-deficient embryos showed an overgrowth of endothelial cells and disorganization of blood vessels (8). Moreover, *Flt-1* tyrosine kinase-deficient mice showed normal vascular development (9), suggesting that the Flt-1 extracellular domain acts as a negative regulator of VEGF, and that Flt-1 tyrosine kinase is not necessary for vasculogenesis during development. On the other hand, *Flk-1*-deficient mice lack both mature endothelial and hematopoietic cells, indicating that Flk-1 is crucial for vascular development (10).

Ligand binding to Flk-1/KDR induces autophosphorylation of Flk-1/KDR intracellular tyrosine residues and activates several signaling pathways, leading to cell proliferation, survival, migration, and permeability (11). Recently, we have shown that tyrosine residues 1175 (Y1175) and Y1214, but not Y801, on KDR are highly autophosphorylated in response to VEGF, and that Y1175 is crucial for VEGF-dependent cell proliferation via the phospholipase Cγ (PLCγ)/PKC/mitogen-activated protein kinase (MAPK) pathway in cultured endothelial cells (12). However, the importance of these tyrosine residues in Flk-1/KDR *in vivo* remains to be elucidated.

To develop a pharmaceutical drug(s) that efficiently suppresses angiogenesis in diseases such as cancer, it is important to identify the tyrosine residue(s) that is involved in the critical signaling pathway via Flk-1/KDR for *in vivo* angiogenesis. Therefore, in this study, we generated knock-in mice substituting Y1173 (corresponding to Y1175 in human KDR) and Y1212 (Y1214 in KDR) of the *Flk-1* gene with phenylalanine. *Flk-1*^{1173F} homozygous mice showed a severe phenotype and died at E8.5–E9.5 because of defects of endothelial and hematopoietic cells very similar to *Flk-1* null mice. In contrast, *Flk-1*^{1212F} homozygous mice were viable and fertile. These results indicate that Y1173 is essential for the Flk-1 functions both on blood vessel formation and hematopoiesis during mouse embryogenesis.

Materials and Methods

Construction of Targeting Vector. Genomic fragments containing exons 13–28 of mouse *Flk-1* gene were isolated from a mouse 129Sv genomic library (Stratagene). Site-directed mutagenesis was performed on a 0.65-kb *Nco*I–*Eco*RI fragment containing exon 27, introducing the substitution mutations Y1173F (TAT → TTC) and Y1212F (TAT → TTC). To distinguish the wild-type allele and mutant allele by restriction enzyme digestion, restriction sites were also introduced near the Y1173F and Y1212F mutations without changing the coding amino acids. In the Y1173F targeting vector, the *Acc*III restriction site was introduced at position S1188 (TCT → TCC). In the Y1212F targeting vector, the *Pvu*II restriction site was introduced at position A1216 (GCA → GCT). In both targeting vectors, a *loxP*-flanked *neomycin* (*neo*) resistance gene (pMC1-NeopolyA) was inserted at an *Nco*I site in intron 26, and a diphtheria toxin A subunit gene (pMC1-DT-A) was inserted at the 3′ terminus of the targeting vectors. An *Nco*I site in intron 25 in the targeting vector was destroyed accidentally by deletion of a single nucleotide. The mutations and the nucleotide sequences at exons 19–27 in the targeting constructs were confirmed by DNA sequencing.

Generation of Mutant Mice. The targeting vectors were linearized with *Not*I and transfected into 129 E14 embryonic stem (ES) cells by electroporation. ES cell clones were selected with 400 μg/ml G418 and screened by Southern blotting. For Southern blotting, genomic DNA was digested with *Bgl*II for 3′ probe and *neo* probe and also digested with *Nco*I for 5′ probe and *neo* probe. The mutations of ES clones were confirmed by sequencing. Each ES cell clone correctly targeted for Y1173F and Y1212F was injected into C57BL/6J blastocysts, and the chimeras were mated with C57BL/6J females. For deletion of the *neo*-resistance gene, *Flk-1*^{1173Fneo} and *Flk-1*^{1212Fneo} heterozygous males were mated with CAG-*cre* transgenic (13) females. Deletion of the *neo* gene was confirmed by Southern blotting. *Flk-1*^{1173F} and *Flk-1*^{1212F} heterozygous mice were then intercrossed to generate homozygous mutant mice. Mice were genotyped by Southern blotting and genomic PCR. Full-length mRNA sequences of *1173F*-mutated *Flk-1* and *1212F*-mutated *Flk-1* were confirmed by sequencing analysis with mRNAs from E8.5 *Flk-1*^{1173F} or *Flk-1*^{1212F} homozygous embryos. *Flk-1* knockout mice (10) were purchased from The Jackson Laboratory.

Western Blotting. Lung tissues of adult mice were lysed in 1% Triton X-100 lysis buffer (50 mM Hepes, pH 7.4/150 mM NaCl/10% glycerol/1 mM PMSF/2% Trasylol), using a homogenizer. The lysates were clarified by centrifugation and subjected to SDS/

This paper was submitted directly (Track II) to the PNAS office.

Abbreviations: E*n*, embryonic day *n*; MAPK, mitogen-activated protein kinase; PECAM-1, platelet endothelial cell adhesion molecule 1; PLCγ, phospholipase Cγ.

‡To whom correspondence should addressed. E-mail: shibuya@ims.u-tokyo.ac.jp.

© 2005 by The National Academy of Sciences of the USA

www.pnas.org/cgi/doi/10.1073/pnas.0404984102

Downloaded from https://www.pnas.org by 18.97.14.90 on February 10, 2025 from IP address 18.97.14.90.

PAGE. Proteins were then transferred to a poly(vinylidene difluoride) membrane (Millipore). Membranes were blotted by using anti-Flk1 antibody (rabbit polyclonal antisera generated against a synthetic peptide of KDR/Flk-1, residues 1294–1316) (14) and mouse anti-actin monoclonal antibody (MAB1501, Chemicon). Protein bands were visualized by using the ECL detection system (Amersham Pharmacia).

RT-PCR Analysis. Total RNA was isolated from E8.5 embryos including yolk sacs by using ISOGEN (Nippon Gene, Tokyo). Reverse transcription was performed with an M-MLV reverse transcriptase (Life Technologies) and random hexamers according to the manufacturer's instructions. Primers for PCR amplification of *Flk-1* in Fig. 1*D* were 5′-TTGGAGCATCTCATCTGTTACAGC-3′ and 5′-GGCCGGCTCTTTCGCTTACT-3′. After *Acc*III digestion of the PCR products (695 bp), the products from the wild-type allele were not digested (695 bp), but the products from the *1173F* mutant allele were digested into 567- and 128-bp bands. Primers for Fig. 5*A* were designed as follows: *Flk-1*, 5′-GAGAGCAAGGCGCTGCTAGC-3′, 5′-GACAGAGGCGATGAATGGTG-3′; *Flt-1*, 5′-ATTATGGACCCAGATGAAGT-3′, 5′-TCACAGCCACAGTCCGGCAG-3′; *Tie-1*, 5′-ACCCACTACCAGCTGGATGT-3′, 5′-ATCGTGTGCTAGCATTGAGG-3′; *Tie-2*, 5′-CCACTACCTACTAGTGAAG-3′, 5′-ATGCCCTTCTCCACCCTCT-3′; *CD34*, 5′-GTTACCTCTGGGATCCCTTCAGGCTC-3′, 5′-CTCCAGAGGTGACCAATGCAATAAG-3′; *βH1*, 5′-AGTCCCCATGGAGTCAAAGA-3′, 5′-CTCAAGGAGACCTTTGCTCA-3′; *β-actin*, 5′-TCGTGCGTGACATCAAAGAG-3′, 5′-TGGACAGTGAGGCCAGGATG-3′.

Whole-Mount Immunohistochemistry. For whole-mount immunostaining of platelet endothelial cell adhesion molecule 1 (PECAM-1) and Flk-1, embryos were fixed in 2% paraformaldehyde in PBS for 20 min at 4°C. The fixed embryos were rinsed in PBS, dehydrated in a methanol series, and stored in 100% methanol at −20°C until use. To block endogenous peroxidase, the dehydrated embryos were bleached in methanol containing 0.3% H_2O_2 for 30 min at 4°C. The bleached embryos were rehydrated and blocked in PBSMT (2% skim milk and 0.3% Triton X-100 in PBS) containing 0.2% BSA for 1 h twice at room temperature. The embryos were then incubated with PBSMT containing anti-PECAM-1 monoclonal antibody (clone MEC13.3, Pharmingen) or anti-Flk-1 monoclonal antibody (clone Avas 12α1, Pharmingen) overnight at 4°C. After washing five times in PBSMT each for 1 h at 4°C (initial three times) and room temperature (final two times), the embryos were incubated with HRP-conjugated anti-rat Ig antibody (BioSource International, Camarillo, CA) in PBSMT overnight at 4°C. After extensive washing with more than five exchanges of PBSMT, including the final 20-min wash in PBST (0.3% Triton X-100 in PBS) at room temperature, embryos were incubated with 0.3 mg/ml DAB in PBST for 20 min at room temperature, then H_2O_2 was added to a final concentration of 0.0075%. The staining reaction was stopped by rinsing in PBST.

LacZ Staining. For whole-mount LacZ staining, embryos were fixed in a fixing solution (0.2% glutaraldehyde/1% formaldehyde/0.02% Nonidet P-40 in PBS) for 30 min at 4°C. After washing with PBS for 20 min at room temperature twice, the embryos were incubated in X-gal staining solution [5 mM $K_3Fe(CN)_6$/5 mM $K_4Fe(CN)_6$/2 mM $MgCl_2$/1 mg/ml X-gal in PBS] overnight at room temperature. The embryos were then washed with PBS three times each for 20 min at room temperature. For sections, the LacZ stained embryos were fixed in 3.7% formaldehyde-PBS and embedded in paraffin. The embryos were then sectioned and counterstained with eosin.

Hematopoietic Colony Assay. E8.5 embryos including yolk sacs were treated with 0.1% collagenase/20% FBS in PBS for 30 min at 37°C with occasional agitation. After incubation, the cells were washed with 20% FBS in PBS, then plated in 1% methylcellulose/Iscove's MDM containing 15% FBS, 10 μg/ml insulin, 50 ng/ml stem cell factor (SCF), 10 ng/ml IL-3, 10 ng/ml IL-6, and 3 units/ml erythropoietin (Methocult GF M3434, Stem Cell Technologies, Vancouver). The numbers of erythroid colonies, granulocyte/macrophage colonies, and mixed colonies were counted after 7 days of culture.

Results

To examine the role of Flk-1 tyrosine residues *in vivo*, we generated knock-in mice substituting Y1173 and Y1212 of the *Flk-1* gene with phenylalanine. Point mutations were introduced in exon 27 of the *Flk-1* gene (Fig. 1*A*). In addition, to distinguish the mutant mRNA from the wild-type mRNA, nucleotide substitutions were introduced in the mutant allele for generation of an *Acc*III site in *Y1173F* mutants or a *Pvu*II site in *Y1212F* mutants without any change in amino acid levels. The *neo*-resistance gene was flanked by two *loxP* sites and deleted by crossing heterozygous mutant mice with CAG-*cre* transgenic mice (13). The generation of mutant mice was confirmed by Southern blotting of tail genomic DNA (Fig. 1*B*). Although *Flk-1*^{1173F} heterozygous (*Flk-1*$^{+/1173F}$) mice were normal, no *Flk-1*^{1173F} homozygotes (*Flk-1*$^{1173F/1173F}$) survived among 128 newborn animals from *Flk-1*$^{+/1173F}$ crosses, indicating that *Flk-1*$^{1173F/1173F}$ mice died *in utero* (Table 1). At embryonic stages, *Flk-1*$^{1173F/1173F}$ embryos were similar in size to their wild-type and heterozygous littermates at E8.5 but clearly abnormal at E9.5. At E10.5, *Flk-1*$^{1173F/1173F}$ embryos were necrotic and mostly resorbed. These results suggest that *Flk-1*$^{1173F/1173F}$ embryos died between E8.5 and E9.5, very similar to *Flk-1* null mice (10). In contrast, crossing of *Flk-1*^{1212F} heterozygous mice yielded homozygous offspring at Mendelian ratios (Table 1). The *Flk-1*^{1212F} homozygous (*Flk-1*$^{1212F/1212F}$) mice were viable and fertile.

Flk-1 protein expression in these mice was analyzed by Western blotting. The expression level of Flk-1 in adult lung lysates was almost the same among the wild-type, *Flk-1*$^{+/1173F}$, *Flk-1*$^{+/1212F}$, and *Flk-1*$^{1212F/1212F}$ mice (Fig. 1*C*). Moreover, in the *Flk-1*^{1212Fneo} heterozygous and homozygous mice that still carry the *neo* gene, the expression level of Flk-1 was comparable to that of wild-type mice (Fig. 1*C*). Although these results suggest that the *neo* gene does not significantly suppress the expression of *Flk-1* gene, to avoid any effect of *neo* gene on gene expression, the following experiments were done by using *neo*-gene-removed knock-in mice. Because *Flk-1*$^{1173F/1173F}$ mice died at E8.5–E9.5, the expression level of 1173F-mutant Flk-1 was analyzed by RT-PCR with E8.5 embryos (Fig. 1*D*). To distinguish mRNA from wild-type alleles and *1173F* mutant alleles, RT-PCR products were digested with *Acc*III, which digests only the *1173F* mutant PCR product. In *Flk-1*$^{+/1173F}$ mice, the density of the 695-bp band from the wild-type allele was almost the same as that of the digested 567-bp band from *1173F* mutant allele, indicating that the mRNA expression from the *1173F* mutant allele was basically normal.

To further analyze the role of Flk-1 Y1173 during mouse development, the phenotypes of *Flk-1*$^{1173F/1173F}$ and *Flk-1* null knockout (*Flk-1*$^{KO/KO}$) mice were compared. Fig. 2 shows the morphological comparison between the wild-type, *Flk-1*$^{1173F/1173F}$, and *Flk-1*$^{KO/KO}$ embryos. At E9.5, *Flk-1*$^{1173F/1173F}$ and *Flk-1*$^{KO/KO}$ embryos were smaller than wild-type embryos, and blood vessels were absent both in the embryos and yolk sacs of *Flk-1*$^{1173F/1173F}$ and *Flk-1*$^{KO/KO}$ mice (Fig. 2 *A–C*). To visualize the endothelial cells, we performed whole-mount immunostaining of E8.5 (Fig. 2 *D–F*) and E9.5 (Fig. 2 *G–I*) embryos with the endothelial marker anti-PECAM-1 antibody. PECAM-1-positive blood vessels were clearly visible in embryos and yolk sacs of wild-type mice (Fig. 2 *D* and *G*) but completely absent in those of *Flk-1*$^{1173F/1173F}$ (Fig. 2 *E* and *H*) and *Flk-1*$^{KO/KO}$ (Fig. 2 *F* and *I*) mice. Flk-1 expression was also examined by whole-mount

Downloaded from https://www.pnas.org by 18.97.14.90 on February 10, 2025 from IP address 18.97.14.90.

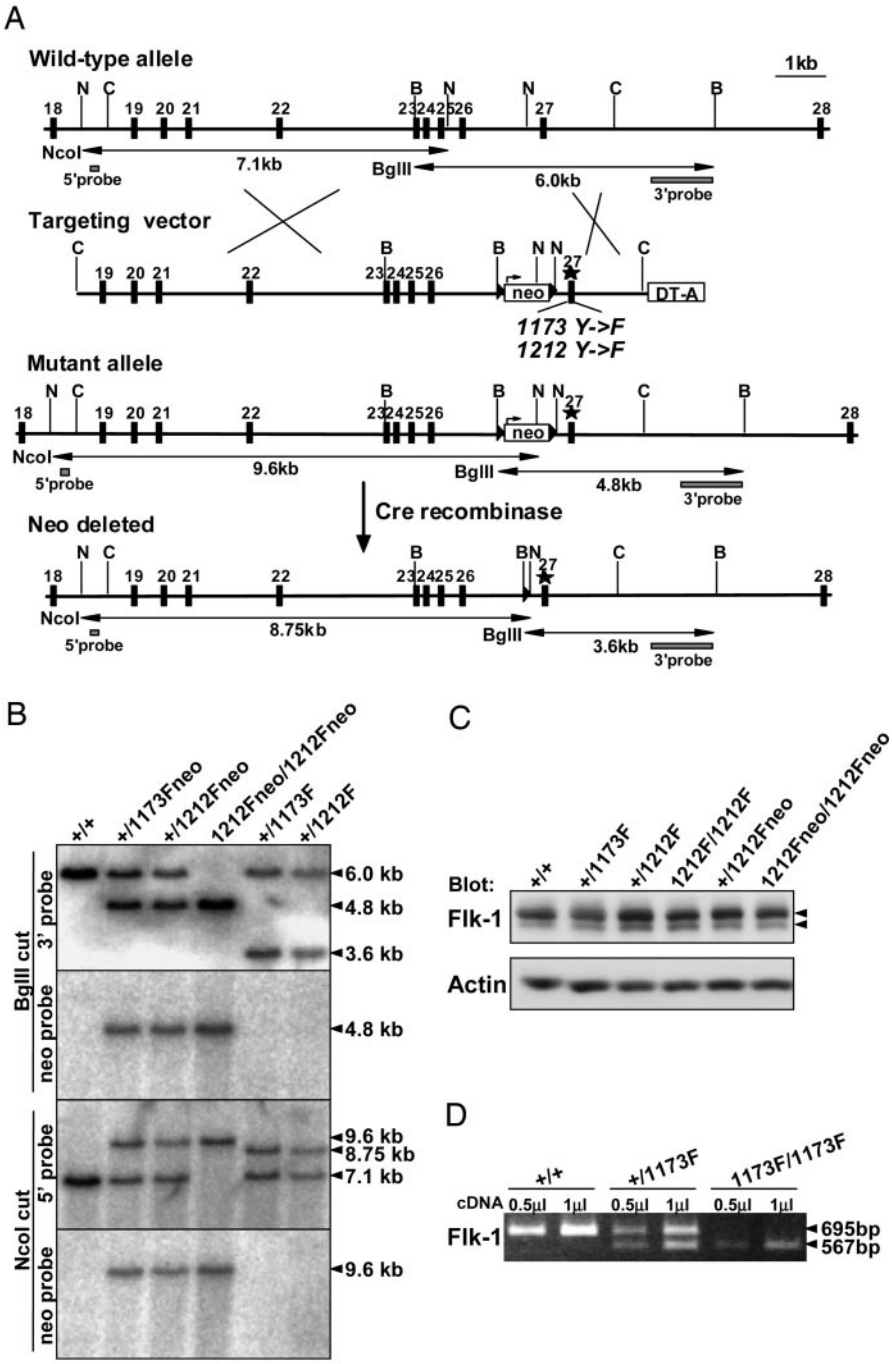

Fig. 1. Generation of *Flk-1* knock-in mutant mice. (*A*) Targeting strategy. B, *Bgl*II; C, *Cla*I; N, *Nco*I. *LoxP* sites are indicated by triangles. (*B*) Southern blot analysis of tail genomic DNA from wild-type (+/+), *Flk-1*$^{+/1173Fneo}$, *Flk-1*$^{+/1212Fneo}$, *Flk-1*$^{1212Fneo/1212Fneo}$, *Flk-1*$^{+/1173F}$, and *Flk-1*$^{+/1212F}$ mice. Tail genomic DNA was digested with *Bgl*II and hybridized with a 3′ probe and *neo* probe, or digested with *Nco*I and hybridized with a 5′ probe and *neo* probe. (*C*) Western blotting of lung lysates from adult mice with anti-Flk-1 antibody. Arrowheads indicate Flk-1 proteins. Anti-actin antibody was used as a control to verify that an equivalent amount of protein was loaded in each lane. (*D*) RT-PCR analysis of wild-type (+/+), *Flk-1*$^{+/1173F}$, and *Flk-1*$^{1173F/1173F}$ E8.5 embryos. PCR was performed by using 0.5 μl or 1 μl of cDNA in 20-μl reactions by *Flk-1* primers coding exons 22–28. The PCR products were digested with *Acc*III, which digests only the *1173F* mutant PCR products. The undigested, 695-bp product represents the mRNA expressed from the wild-type allele, and the digested 567-bp product represents the mRNA expressed from the *1173F* mutant allele.

immunostaining with anti-Flk-1 antibody at E8.5 (Fig. 2 *J–L*) and E9.5 (Fig. 2 *M–O*) embryos. *Flk-1*$^{KO/KO}$ embryos were not stained by anti-Flk-1 antibody because of the lack of Flk-1 protein expression (Fig. 2 *L* and *O*). In contrast, weak but clear Flk-1 staining was detected in *Flk-1*$^{1173F/1173F}$ embryo bodies but not in the yolk sacs (Fig. 2 *K* and *N*), indicating that Flk-1 1173F mutant proteins were expressed in *Flk-1*$^{1173F/1173F}$ embryos. However, the Flk-1-positive blood vessels which were clearly detectable in wild-type mice (Fig. 2 *J* and *M*) were not observed in *Flk-1*$^{1173F/1173F}$ mice (Fig. 2 *K* and *N*). These results show that the cells expressing Flk-1 1173F mutant proteins are present, but mature endothelial cells are absent, in *Flk-1*$^{1173F/1173F}$ embryos.

We further compared the phenotypes of *Flk-1* null and *Flk-1*^{1173F} mutant embryos by LacZ staining. In *Flk-1* null mutant mice, the

Downloaded from https://www.pnas.org by 18.97.14.90 on February 10, 2025 from IP address 18.97.14.90.

Table 1. Analysis of genotypes obtained from heterozygote crosses

Stages	No. tested	+/+	+/F	F/F
	Flk-1^{1173F} (F) heterozygote crosses			
E8.5	107	25	54	28
E9.5	11	2	6	3*
E10.5	18	4	7	7†
E12.5	16	8	8	0
E14.5	10	5	5	0
E16.5	10	7	3	0
Adult	128	46	82	0
	Flk-1^{1212F} (F) heterozygote crosses			
E8.5	11	3	5	3
Adult	155	30	82	43

*Morphologically abnormal embryos.
†Necrotic embryos.

LacZ gene was inserted under the transcriptional control of the endogenous *Flk-1* promoter (10). *Flk-1*$^{KO/1173F}$ embryos, which have the *LacZ* gene and express only 1173F-mutant Flk-1 proteins, were compared with *Flk-1*$^{KO/KO}$ embryos. At E8.5, LacZ expression was detected in *Flk-1*$^{KO/1173F}$ (Fig. 3*B*) and *Flk-1*$^{KO/KO}$ (Fig. 3*C*) embryo bodies and allantois, but blood vessels such as the dorsal aorta and yolk sac vasculature detected in *Flk-1*$^{+/KO}$ (Fig. 3*A*) embryos were not observed in either *Flk-1*$^{KO/1173F}$ or *Flk-1*$^{KO/KO}$ embryos.

Blood vessel organization was further examined by sections of LacZ-stained E8.5 embryos (Fig. 3 *D–R*). Blood vessels in the head region were observed only in *Flk-1*$^{+/KO}$ embryos (Fig. 3*D*), not in *Flk-1*$^{KO/1173F}$ (Fig. 3*E*) or *Flk-1*$^{KO/KO}$ (Fig. 3*F*) embryos,

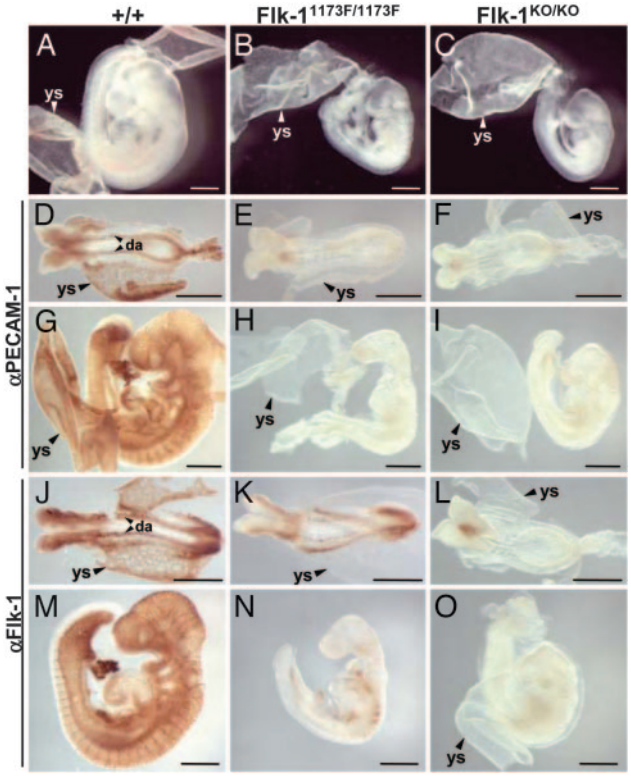

Fig. 2. Blood vessels are absent in *Flk-1*$^{1173F/1173F}$ embryos. (*A–C*) Morphology of E9.5 wild-type (*A*), *Flk-1*$^{1173F/1173F}$ (*B*), and *Flk-1*$^{KO/KO}$ (*C*) embryos. (*D–I*) Whole-mount PECAM-1 immunostaining of E8.5 (*D–F*) and E9.5 (*G–I*) embryos. (*J–O*) Whole-mount Flk-1 immunostaining of E8.5 (*J–L*) and E9.5 (*M–O*) embryos. da, dorsal aorta; ys, yolk sac. (Scale bars: 500 μm.)

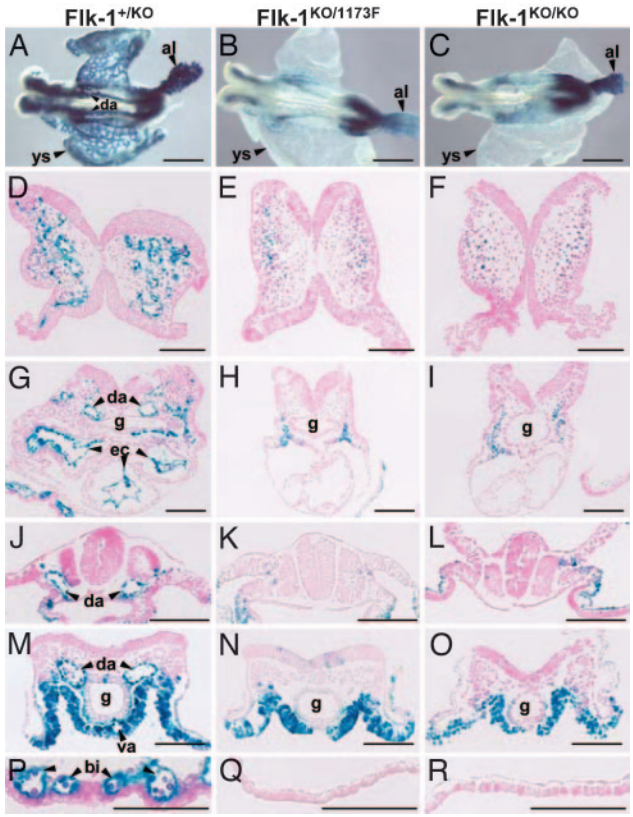

Fig. 3. LacZ staining of E8.5 *Flk-1*$^{+/KO}$, *Flk-1*$^{KO/1173F}$, and *Flk-1*$^{KO/KO}$ embryos. (*A–C*) Whole-mount LacZ staining. (*D–R*) Transverse sections of LacZ-stained embryos. (*D–F*) Head region. (*G–I*) Heart region. (*J–L*) Somatic region. (*M–O*) Tail region. (*P–R*) Yolk sac. al, allantois; bi, blood island; da, dorsal aorta; ec, endocardium; g, gut; va, vitelline artery; ys, yolk sac. (Scale bars: *A–C*, 500 μm; *D–R*, 100 μm.)

although LacZ-positive cells were present to some extent in the head mesenchyme tissue in all embryos. In the heart region, LacZ-stained endocardium that was found in *Flk-1*$^{+/KO}$ embryos (Fig. 3*G*) was not detected in either *Flk-1*$^{KO/1173F}$ (Fig. 3*H*) or *Flk-1*$^{KO/KO}$ (Fig. 3*I*) embryos. LacZ-positive cells were seen at the sides of the gut in the heart and tail regions of *Flk-1*$^{KO/1173F}$ (Fig. 3 *H* and *N*) and *Flk-1*$^{KO/KO}$ (Fig. 3 *I* and *O*) embryos. However, the dorsal aorta and vitelline artery that were seen in the heart, somite, and tail regions of *Flk-1*$^{+/KO}$ embryos (Fig. 3 *G*, *J*, and *M*) were not found in those regions of *Flk-1*$^{KO/1173F}$ (Fig. 3 *H*, *K*, and *N*) and *Flk-1*$^{KO/KO}$ (Fig. 3 *I*, *L*, and *O*) embryos. Moreover, yolk sac blood islands that were clearly detectable in *Flk-1*$^{+/KO}$ yolk sacs (Fig. 3*P*) were entirely absent in *Flk-1*$^{KO/1173F}$ (Fig. 3*Q*) and *Flk-1*$^{KO/KO}$ (Fig. 3*R*) yolk sacs. In addition, round cells looking like hematopoietic cells found in sections of *Flk-1*$^{+/KO}$ embryos were also not observed in *Flk-1*$^{KO/1173F}$ and *Flk-1*$^{KO/KO}$ embryos, suggesting a defect in hematopoietic development.

To further analyze the defects of endothelial and hematopoietic cells, we examined E7.5 embryos by LacZ staining (Fig. 4 *A–I*), because both endothelial and hematopoietic lineages first arise in yolk sac blood islands in this stage. At E7.5, blood islands were clearly detectable within the extraembryonic mesoderm of yolk sacs in *Flk-1*$^{+/KO}$ embryos (Fig. 4 *A*, *D*, and *G*). In contrast, in *Flk-1*$^{KO/1173F}$ (Fig. 4 *B*, *E*, and *H*) and *Flk-1*$^{KO/KO}$ (Fig. 4 *C*, *F*, and *I*) embryos, blood islands in the yolk sacs were completely absent, and the extraembryonic mesoderm consisted of a single cell layer. In *Flk-1*$^{KO/1173F}$ and *Flk-1*$^{KO/KO}$ embryos, LacZ-positive cells were mainly detected in the allantois and the mesodermal component of

Downloaded from https://www.pnas.org by 18.97.14.90 on February 10, 2025 from IP address 18.97.14.90.

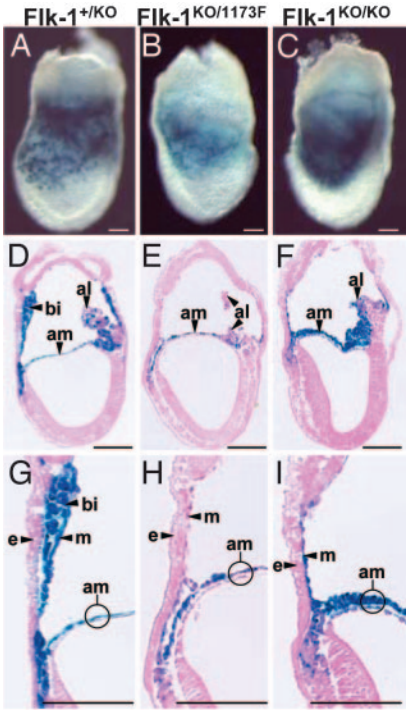

Fig. 4. LacZ staining of E7.5 *Flk-1*$^{+/KO}$, *Flk-1*$^{KO/1173F}$, and *Flk-1*$^{KO/KO}$ embryos. (*A–C*) Whole-mount LacZ staining. (*D–I*) Sagittal sections of LacZ-stained embryos. (*G–I*) Higher magnification of *D–F*. al, allantois; am, amnion; bi, blood island; e, endoderm; m, mesothelium. (Scale bars: 100 μm.)

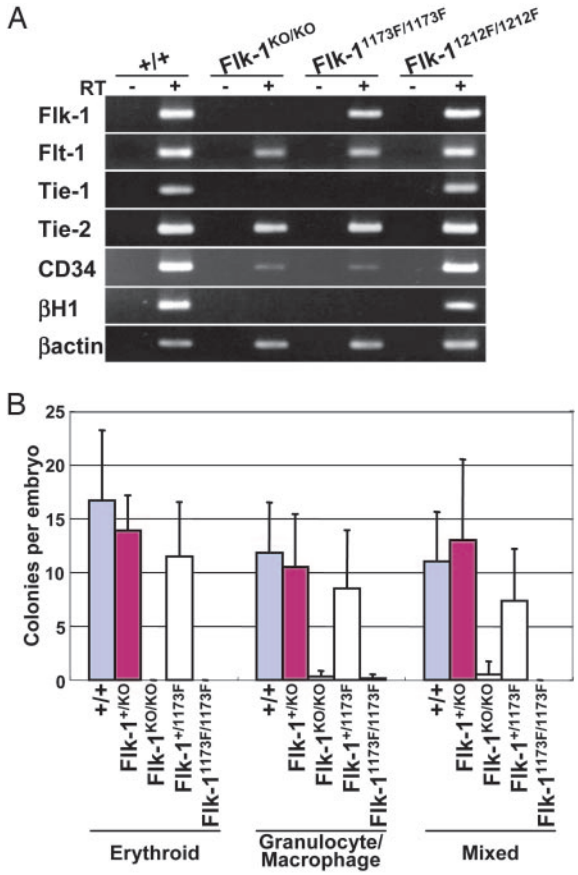

Fig. 5. Hematopoietic defects in *Flk-1*$^{1173F/1173F}$ embryos. (*A*) RT-PCR analysis of *Flk-1*, *Flt-1*, *Tie-1*, *Tie-2*, *CD34*, and *βH1* with E8.5 wild-type, *Flk-1*$^{KO/KO}$, *Flk-1*$^{1173F/1173F}$, and *Flk-1*$^{1212F/1212F}$ embryos including yolk sacs. Each amplification was performed in the absence (−) or presence (+) of reverse transcriptase (RT) to detect genomic DNA contamination. *β-actin* was used as a positive control. (*B*) Hematopoietic colony formation assay of E8.5 wild-type, *Flk-1*$^{+/KO}$, *Flk-1*$^{KO/KO}$, *Flk-1*$^{+/1173F}$, and *Flk-1*$^{1173F/1173F}$ embryos including yolk sacs. Error bars indicate the standard deviation. Wild-type, $n = 6$; *Flk-1*$^{+/KO}$, $n = 8$; *Flk-1*$^{KO/KO}$, $n = 6$; *Flk-1*$^{+/1173F}$, $n = 8$; *Flk-1*$^{1173F/1173F}$, $n = 7$.

amnion, in which region *Flk-1*$^{+/KO}$ embryos also have LacZ expression. These results show that the LacZ expression pattern and the deficiency of blood vessels of *Flk-1*$^{KO/1173F}$ embryos are basically identical to those of *Flk-1*$^{KO/KO}$ embryos, indicating that the phenotype of *Flk-1*^{1173F} mutant mice is very similar to that of *Flk-1* null mice.

Next, the expression of endothelial markers and hematopoietic markers were analyzed by RT-PCR using E8.5 wild-type, *Flk-1*$^{KO/KO}$, *Flk-1*$^{1173F/1173F}$, and *Flk-1*$^{1212F/1212F}$ embryos including yolk sacs (Fig. 5*A*). In *Flk-1*$^{1212F/1212F}$ embryos, all markers were expressed normally. As expected, *Flk-1* mRNA was not expressed in *Flk-1*$^{KO/KO}$ embryos. In *Flk-1*$^{1173F/1173F}$ embryos, the *Flk-1* expression was reduced compared with wild-type embryos, consistent with the weak signal in Flk-1 immunostaining as shown in Fig. 2. In terms of endothelial markers, *Flt-1* and *Tie-2* were expressed in all embryos, but *Tie-1* was not expressed in either *Flk-1*$^{KO/KO}$ or *Flk-1*$^{1173F/1173F}$ embryos. These results suggest the presence of endothelial precursors, but no mature endothelial cells, in *Flk-1*$^{KO/KO}$ or *Flk-1*$^{1173F/1173F}$ embryos. The expression of *CD34*, which is expressed in hematopoietic stem cells and endothelial cells, was greatly reduced in *Flk-1*$^{KO/KO}$ and *Flk-1*$^{1173F/1173F}$ embryos. Embryonic β-globin, *βH1*, was not expressed in either *Flk-1*$^{KO/KO}$ or *Flk-1*$^{1173F/1173F}$ embryos, suggesting that primitive erythrocytes were absent in these mice.

To examine the presence of hematopoietic progenitors, a methylcellulose colony formation assay was performed by using E8.5 embryos including yolk sacs (Fig. 5*B*). The number of erythroid, granulocyte/macrophage, and mixed colonies were counted after 7 days of culture. As a result, the colonies from *Flk-1*$^{KO/KO}$ or *Flk-1*$^{1173F/1173F}$ mice were not observed or were greatly reduced compared with those from wild-type mice, although the number of colonies from *Flk-1*$^{+/KO}$ and *Flk-1*$^{+/1173F}$ mice was not significantly different from that of wild-type mice. These results indicate that in addition to the lack of mature hematopoietic cells, hematopoietic progenitors are also severely reduced in *Flk-1*$^{KO/KO}$ and *Flk-1*$^{1173F/1173F}$ mice.

We previously showed that Y1175 of KDR (corresponding to Y1173 in murine Flk-1) is important for VEGF-dependent MAPK activation in cultured endothelial cells (12). To determine the role of Flk-1 Y1173 for MAPK activation in mouse embryo, we performed whole-mount immunostaining of E8.5 embryos with anti-phospho-MAPK antibody, which recognizes activated MAPK (Fig. 6 and *Supporting Materials and Methods*, which are published as supporting information on the PNAS web site). To confirm the specificity of staining, embryos were incubated with a MEK (MAPK kinase) inhibitor, U0126. As a result, phospho-MAPK staining was significantly decreased in U0126-treated embryos (Fig. 6*H*) compared with DMSO control (Fig. 6*F*), indicating that the staining was specific to the phosphorylated form of MAPK. However, staining in *Flk-1*$^{1173F/1173F}$ embryos (Fig. 6*D*) did not significantly differ from that in *Flk-1*$^{+/1173F}$ (Fig. 6*B*) or wild-type (data not shown) embryos, although some *Flk-1*$^{1173F/1173F}$ embryos showed slightly reduced staining (data not shown). Because VEGF receptor inhibitor KRN633 did not clearly diminish phospho-MAPK staining (Fig. 6*J*), most of the MAPK activation may not depend on Flk-1 at this stage.

Discussion

To date, several Flk-1/KDR intracellular tyrosine residues have been identified as autophosphorylation sites (15–19). Dougher-

Downloaded from https://www.pnas.org by 18.97.14.90 on February 10, 2025 from IP address 18.97.14.90.

Vermazen *et al.* (15) reported that in a bacteria expression system, Y951, Y996, Y1054, and Y1059 on KDR were phosphorylated. On the other hand, Cunningham *et al.* (16) reported that in the yeast system, Y801 and Y1175 on KDR were phosphorylated. The role of these tyrosine residues for Flk-1/KDR-mediated signal transduction remains controversial. Y1054 and Y1059, which are located in the KDR kinase domain, were reported to be required for VEGF-dependent maximal KDR kinase activity when the Y1054F/Y1059F-mutant KDR was overexpressed in 293 cells (17). Zeng *et al.* (19) reported that Y951 and Y1059 were important for KDR-mediated human umbilical vein endothelial cell migration and proliferation, respectively, using EGF receptor/KDR chimeric receptors. However, these results were obtained from *in vitro* culture experiments, not from *in vivo* studies. Furthermore, Y1059F mutant might directly suppress the tyrosine kinase activity because this residue is located in the critical region of the kinase domain.

In this study, we demonstrated that *Flk-1^{1173F}* mutant mice die at E8.5–E9.5 because of defects of endothelial and hematopoietic cells very similar to those in *Flk-1* null mice. We and other group previously showed that the substitution of Y1173 on Flk-1 (Y1175 on KDR) with phenylalanine does not affect the level of autophosphorylation of Flk-1/KDR or the stability of Flk-1/KDR in cultured endothelial cells (12, 18). Therefore, the phenotype of *Flk-1^{1173F}* mutant mice does not appear to be due to the inactivation of Flk-1 kinase. Moreover, a ratio of the Flk-1 protein level between wild-type (Fig. 2*J*) and *Flk-1$^{1173F/1173F}$* (Fig. 2*K*) mice shown by Flk-1 immunostaining was almost the same as the ratio of LacZ expression level between *Flk-1$^{+/KO}$* (Fig. 3*A*) and *Flk-1$^{KO/1173F}$* (Fig. 3*B*) mice, reflecting the *Flk-1* mRNA level. This similar ratio indicates that the half-life of Flk-1 protein was not significantly altered by mutation of Y1173. Taken together, these results suggest that signaling via Y1173 is essential for Flk-1 functions during mouse embryogenesis. Recently, we showed that Y1175 of KDR (corresponding to Y1173 in Flk-1) is a binding site of PLCγ and is important for VEGF-dependent PLCγ/PKC/MAPK activation leading to DNA synthesis in cultured endothelial cells (12). Accordingly, it is strongly suggested that blood-vessel defects in *Flk-1^{1173F}* mutant mice are caused by the lack of Flk-1-mediated PLCγ/PKC/MAPK activation. Consistent with this idea, it is reported that *PLCγ1* null mice die at approximately E9.0 because of the absence of vasculogenesis and erythrogenesis, similar to *Flk-1* null mice (20, 21). Furthermore, recent analysis of zebrafish mutants demonstrated that PLCγ1 is required for the function of VEGF and arterial development, indicating that PLCγ1 plays a crucial role in the downstream signaling of the VEGF receptor during embryogenesis in zebrafish (22). MAPK activation was analyzed by immunostaining with phospho-MAPK antibody (Fig. 6), but staining in *Flk-1$^{1173F/1173F}$* embryos was not clearly reduced. Because *Flk-1$^{KO/KO}$* embryos also showed a staining pattern similar to that of wild-type embryos (data not shown), MAPK activation at this stage may primarily depend on other receptor(s) such as FGF receptor, as described in ref. 23.

In addition to the PLCγ/PKC/MAPK pathway, several signaling molecules such as phosphatidylinositol 3-kinase (PI3K), Akt, Src, and focal adhesion kinase have been reported to be activated downstream of Flk-1/KDR activation in cultured endothelial cells (11). Very recently, Holmqvist *et al.* (24) reported that the adaptor protein Shb binds to Y1175 in KDR and regulates VEGF-induced PI3K activation and cell migration. Therefore, it is possible that Y1173 on Flk-1 is required not only for the PLCγ/PKC/MAPK pathway but also for additional signaling pathway(s) during mouse embryogenesis.

Our previous study showed that Y1214 (corresponding to Y1212 in Flk-1) is an additional autophosphorylation site of KDR but is not required for VEGF-dependent PLCγ/PKC/MAPK activation or DNA synthesis in cultured endothelial cells (12). Recently, Meyer *et al.* (25) reported that Y1212 of Flk-1 is required for autophosphorylation of Flk-1 and activation of PLCγ1 and MAPK. In this paper, we demonstrated that *Flk-1^{1212F}* mutant homozygous mice are viable and fertile, indicating that Y1212 of Flk-1 is not essential for normal development in mice. However, the role of Flk-1 Y1212 in pathological conditions such as tumor angiogenesis remains to be elucidated.

To date, studies have been reported of several receptors using knock-in mice in which the cytoplasmic tyrosine(s) of a receptor has been replaced with phenylalanine(s) (26–30). However, it is rare that the substitution of a single tyrosine of a receptor causes the same phenotype as the null mutant mice. Platelet-derived growth factor receptor β (PDGFRβ) is another important signal transducer for blood vessel formation and primarily regulates the recruitment and proliferation/differentiation of pericytes. Knock-in studies of PDGFRβ have, however, shown that none of the tyrosine residues for autophosphorylation are crucial but rather provide additive signaling effects (30). Thus, the results obtained regarding *Flk-1^{1173F}* mutant mice in this paper demonstrate that Flk-1 is a unique receptor because of the critical role of a single tyrosine residue for its *in vivo* functions. Taken together, we propose that the phosphorylated tyrosine residue 1173 on Flk-1 in mice (tyrosine 1175 on human KDR) is a previously unrecognized target for the development of antiangiogenic agents.

We thank Dr. J. Miyazaki for supplying CAG-*cre* transgenic mice. This work was supported by Grant-in-Aid Special Project Research on Cancer–Bioscience 12215024 from the Ministry of Education, Culture, Sports, Science, and Technology of Japan, a grant from the program "Research for the Future" of the Japan Society for Promotion of Science, and the program "Promotion of Fundamental Research in Health Science" of the Organization for Pharmaceutical Safety and Research.

1. Shibuya, M. (2001) *Cell Struct. Funct.* **26,** 25–35.
2. Ferrara, N., Gerber, H. P. & LeCouter, J. (2003) *Nat. Med.* **9,** 669–676.
3. Shibuya, M., Yamaguchi, S., Yamane, A., Ikeda, T., Tojo, A., Matsushime, H. & Sato, M. (1990) *Oncogene* **5,** 519–524.
4. de Vries, C., Escobedo, J. A., Ueno, H., Houck, K., Ferrara, N. & Williams, L. T. (1992) *Science* **255,** 989–991.
5. Matthews, W., Jordan, C. T., Gavin, M., Jenkins, N. A., Copeland, N. G. & Lemischka, I. R. (1991) *Proc. Natl. Acad. Sci. USA* **88,** 9026–9030.
6. Terman, B. I., Dougher-Vermazen, M., Carrion, M. E., Dimitrov, D., Armellino, D. C., Gospodarowicz, D. & Bohlen, P. (1992) *Biochem. Biophys. Res. Commun.* **187,** 1579–1586.
7. Millauer, B., Wizigmann-Voos, S., Schnurch, H., Martinez, R., Moller, N. P., Risau, W. & Ullrich, A. (1993) *Cell* **72,** 835–846.
8. Fong, G. H., Rossant, J., Gertsenstein, M. & Breitman, M. L. (1995) *Nature* **376,** 66–70.
9. Hiratsuka, S., Minowa, O., Kuno, J., Noda, T. & Shibuya, M. (1998) *Proc. Natl. Acad. Sci. USA* **95,** 9349–9354.
10. Shalaby, F., Rossant, J., Yamaguchi, T. P., Gertsenstein, M., Wu, X. F., Breitman, M. L. & Schuh, A. C. (1995) *Nature* **376,** 62–66.
11. Cross, M. J., Dixelius, J., Matsumoto, T. & Claesson-Welsh, L. (2003) *Trends Biochem. Sci.* **28,** 488–494.
12. Takahashi, T., Yamaguchi, S., Chida, K. & Shibuya, M. (2001) *EMBO J.* **20,** 2768–2778.
13. Sakai, K. & Miyazaki, J. (1997) *Biochem. Biophys. Res. Commun.* **237,** 318–324.
14. Takahashi, T. & Shibuya, M. (1997) *Oncogene* **14,** 2079–2089.
15. Dougher-Vermazen, M., Hulmes, J. D., Bohlen, P. & Terman, B. I. (1994) *Biochem. Biophys. Res. Commun.* **205,** 728–738.
16. Cunningham, S. A., Arrate, M. P., Brock, T. A. & Waxham, M. N. (1997) *Biochem. Biophys. Res. Commun.* **240,** 635–639.
17. Dougher, M. & Terman, B. I. (1999) *Oncogene* **18,** 1619–1627.
18. Dayanir, V., Meyer, R. D., Lashkari, K. & Rahimi, N. (2001) *J. Biol. Chem.* **276,** 17686–17692.
19. Zeng, H., Sanyal, S. & Mukhopadhyay, D. (2001) *J. Biol. Chem.* **276,** 32714–32719.
20. Ji, Q. S., Winnier, G. E., Niswender, K. D., Horstman, D., Wisdom, R., Magnuson, M. A. & Carpenter, G. (1997) *Proc. Natl. Acad. Sci. USA* **94,** 2999–3003.
21. Liao, H. J., Kume, T., McKay, C., Xu, M. J., Ihle, J. N. & Carpenter, G. (2002) *J. Biol. Chem.* **277,** 9335–9341.
22. Lawson, N. D., Mugford, J. W., Diamond, B. A. & Weinstein, B. M. (2003) *Genes Dev.* **17,** 1346–1351.
23. Corson, L. B., Yamanaka, Y., Lai, K. M. & Rossant, J. (2003) *Development (Cambridge, U.K.)* **130,** 4527–4537.
24. Holmqvist, K., Cross, M. J., Rolny, C., Hagerkvist, R., Rahimi, N., Matsumoto, T., Claesson-Welsh, L. & Welsh, M. (2004) *J. Biol. Chem.* **279,** 22267–22275.
25. Meyer, R. D., Dayanir, V., Majnoun, F. & Rahimi, N. (2002) *J. Biol. Chem.* **277,** 27081–27087.
26. Blume-Jensen, P., Jiang, G., Hyman, R., Lee, K. F., O'Gorman, S. & Hunter, T. (2000) *Nat. Genet.* **24,** 157–162.
27. Kissel, H., Timokhina, I., Hardy, M. P., Rothschild, G., Tajima, Y., Soares, V., Angeles, M., Whitlow, S. R., Manova, K. & Besmer, P. (2000) *EMBO J.* **19,** 1312–1326.
28. Maina, F., Pante, G., Helmbacher, F., Andres, R., Porthin, A., Davies, A. M., Ponzetto, C. & Klein, R. (2001) *Mol. Cell* **7,** 1293–1306.
29. Klinghoffer, R. A., Hamilton, T. G., Hoch, R. & Soriano, P. (2002) *Dev. Cell* **2,** 103–113.
30. Tallquist, M. D., French, W. J. & Soriano, P. (2003) *PLoS Biol.* **1,** 288–299.

Downloaded from https://www.pnas.org by 18.97.14.90 on February 10, 2025 from IP address 18.97.14.90.